

## Langevin dynamics of $A+A$ reactions in one dimension

This article has been downloaded from IOPscience. Please scroll down to see the full text article.

2007 J. Phys.: Condens. Matter 19 065108

(<http://iopscience.iop.org/0953-8984/19/6/065108>)

View [the table of contents for this issue](#), or go to the [journal homepage](#) for more

Download details:

IP Address: 129.252.86.83

The article was downloaded on 28/05/2010 at 16:03

Please note that [terms and conditions apply](#).

# Langevin dynamics of $A + A$ reactions in one dimension

J M Sancho<sup>1</sup>, A H Romero<sup>2</sup>, A M Lacasta<sup>3</sup> and Katja Lindenberg<sup>4</sup>

<sup>1</sup> Departament d'Estructura i Constituents de la Matèria, Facultat de Física, Universitat de Barcelona, Diagonal 647, E-08028 Barcelona, Spain

<sup>2</sup> Cinvestav-Querétaro, Libramiento Norponiente No 2000, Real de Juriquilla, 76230 Querétaro, Qro, Mexico

<sup>3</sup> Departament de Física Aplicada, Universitat Politècnica de Catalunya, Avenida Doctor Marañón 44, E-08028 Barcelona, Spain

<sup>4</sup> Department of Chemistry and Biochemistry 0340 and Institute for Nonlinear Science, University of California, San Diego, La Jolla, CA 92093-0340, USA

Received 1 August 2006

Published 22 January 2007

Online at [stacks.iop.org/JPhysCM/19/065108](http://stacks.iop.org/JPhysCM/19/065108)

## Abstract

We propose a set of Langevin equations of motion together with a reaction rule for the study of binary reactions. Our scheme is designed to address this problem for arbitrary friction  $\gamma$  and temperature  $T$ . It easily accommodates the inclusion of a substrate potential, and it lends itself to straightforward numerical integration. We test this approach on diffusion-limited ( $\gamma \rightarrow \infty$ ) as well as ballistic ( $\gamma = 0$ )  $A + A \rightarrow P$  reactions for which there are extensive exact and approximate theoretical results as well as extensive Monte Carlo results. We reproduce the known results using our integration scheme, and also present new results for the ballistic reactions.

## 1. Introduction

With very few exceptions, even the simplest irreversible bimolecular reactions of the form  $A + A \rightarrow P$ , that is, those where two reactant particles of the same species  $A$  combine to form a product  $P$ , continue to elude exact solution in regimes where the ordinary laws of mass action do not work. The law of mass action for the concentration  $\rho(t)$  of reactant for either reaction,  $d\rho(t)/dt = -k\rho^2(t)$ , leads to a decay law of the form  $\rho(t) \sim t^{-1}$ , often called the 'classical' decay law. While this law works for sufficiently high dimensions, it generally does not work, for instance, for  $d = 1$ , where one observes slower decay laws, called 'anomalous' in the literature. The reasons for the breakdown are usually fairly well understood and are associated with the evolution of non-uniform spatial distributions and/or velocity correlations that reflect the fact that these systems are not well mixed.

That 'it does not work' is of course a very broad statement, since we have not specified the conditions under which the reaction takes place, or the dynamics under which the reactants move. Indeed, there are a number of essentially 'orthogonal' literatures in which these simple

reactions are discussed for very specific sets of conditions, ones that are sometimes chosen precisely because an exact solution is possible under these conditions. Among these are the one-dimensional diffusion-limited annihilation reaction,  $P = \emptyset$ , where it is possible to calculate (for all time) the total concentration of reactant as a function of time,  $\rho(t)$  [1, 2]. Another is the diffusion-limited coalescence reaction  $A + A \rightarrow A$ , where one can calculate  $\rho(t)$  as well as the distribution function of nearest neighbour interparticle distances [3–7]. These two systems have provided benchmarks against which approximate closure schemes of multiparticle distribution function hierarchies in the diffusion-limited regime can be tested [8].

A third scenario that has been heavily investigated involves the ‘opposite’ limit, namely, one in which the particles move ballistically. Here one focuses not only on the concentration  $\rho(t)$  of reactants but also on their velocity distribution and/or its moments. While these studies tend to start from kinetic equations (e.g., the Boltzmann equation) which are themselves uncontrolled and therefore may or may not provide an exact description of the problem, they strive to solve these kinetic equations exactly so that only the starting point is not controlled. For example, one branch of these studies considers the reaction  $A + A \rightarrow \emptyset$  with reactants that have a dichotomic velocity distribution ( $\pm v$ ) which remains intact as pairs of particles react [9, 10, 12, 13]. Another looks at this reaction when the distribution of velocities is continuous [10, 11, 14–19]. In this case the distribution changes with time and the system cools down as faster particles react more rapidly than slower ones. Embellishments of these basic ingredients are plentiful as well, including the consideration of possible parallel fates (e.g., a combination of the  $A + A \rightarrow A$  and  $A + A \rightarrow \emptyset$  reactions as well as a probability that nothing happens upon encounter) [11, 13, 18]. In any case, the results of these studies are then checked against extensive Monte Carlo or molecular dynamics simulations [10, 11, 14–17, 19].

One can think of all of these scenarios as involving particles that move in space according to classical laws of motion in a thermal environment and react upon encounter. In the simplest such representation one can imagine the reactants to be hard sphere particles that do not interact except upon encounter, so that between encounters the equation of motion of each reactant particle in, say, one dimension, might then be the simple Langevin equation

$$m\ddot{x} = -\gamma\dot{x} + \xi(t). \quad (1)$$

Here  $m$  is the mass of the particle, a dot denotes a derivative with respect to time,  $\gamma$  is the coefficient of friction, and  $\xi(t)$  is a white thermal noise that obeys the fluctuation–dissipation relation at temperature  $T$ ,

$$\langle \xi(t)\xi(t') \rangle = 2\gamma k_B T \delta(t - t'). \quad (2)$$

(It is trivial to generalize this to higher dimensions, but here we will focus on motion in one dimension.) One must specify the initial position and velocity distributions of reactants. If the particles have a radius  $R$ , a reaction takes place (or takes place with a probability  $p < 1$ , but here we always take  $p = 1$ ) when two particle centres are a distance  $2R$  apart (see the appendix for a more precise characterization). One must also define exactly what happens upon encounter of two particles; in particular, if there are relevant product particles as in the reaction  $A + A \rightarrow A$ , one must specify a rule for the velocity of the product particle. In any case, a solution to this dynamical portrait would make it possible to calculate the time-dependent reactant concentration and interparticle distribution functions.

Under what conditions would one expect this description to reproduce the specific cases mentioned above? This is a testable proposition which can be checked via numerical integration. Presumably, the diffusion-limited reactions correspond to the high friction limit where the inertial term  $m\ddot{x}$  becomes irrelevant. The ballistic  $A + A \rightarrow \emptyset$  reaction would of course be associated with the case of zero temperature and no friction.

We have undertaken an encompassing programme of research that subsumes these particular situations as special cases, namely, that of exploring the bimolecular reaction dynamics of Langevin particles (both  $A + A$  and  $A + B$ ) as described above over a wide regime of friction and temperature and initial distributions in one and two dimensions. Our programme also incorporates the possible presence of a surface or substrate potential  $V(x)$ , thus generalizing the equation of motion between encounters to

$$m\ddot{x} = -V'(x) - \gamma\dot{x} + \xi(t), \quad (3)$$

where the prime denotes a derivative with respect to  $x$ . Toward this broad goal, in this paper we present partial results that address the conjectured correspondence between the known cases mentioned earlier and our numerical simulation results in the appropriate parameter regimes. We also present results that seem not to have been presented before. Here we focus on the  $A + A$  diffusion-limited and ballistic regimes and show results for reactant densities, velocity distribution features, and nearest neighbour interparticle distribution functions, in the absence of a substrate potential. Results for the unexplored regimes of intermediate and low friction in a thermal environment and for reactions in the presence of a substrate potential for all frictions will be presented elsewhere [20].

Parenthetically but importantly, we acknowledge that the specific reactions  $A + A \rightarrow \emptyset$  and  $A + A \rightarrow A$  are not chosen for their ‘real life’ significance as much as for their relative mathematical tractability. More interesting for real applications are aggregation reactions of the form  $A + A \rightarrow A_2$  or chains of such reactions,  $A_n + A_m \rightarrow A_{n+m}$ . An extensive review of theories of irreversible aggregation reactions can be found in [21].

In section 2 we consider diffusion-limited reactions, for which we compare results obtained from our numerical integration scheme with exact solutions. These comparisons cover all times rather than just the asymptotic behaviour. In section 3 we present our integration results for ballistic reactions with dichotomic and with continuous (Gaussian) velocity distributions. Here there are no exact results to compare to, but some asymptotic and previous numerical results are available. Our results include distribution functions that to our knowledge have not been previously reported. We conclude with a summary in section 4.

## 2. Diffusion-limited reactions

Diffusion-limited binary reactions are usually characterized by position-dependent concentrations  $\rho(x, t)$  and two-particle distribution functions or nearest neighbour interparticle distance distribution functions. For the reactions of interest here it is observed that initially random distributions of reactants evolve into spatially non-random distributions, and that as a result the global concentration  $\rho(t) \equiv \int_{-\infty}^{\infty} dx \rho(x, t)$  decays anomalously with time, i.e., with a non-classical exponent. To determine these quantities analytically, it is customary to start with a reaction–diffusion equation for  $\rho(x, t)$  in which the reaction term involves a two-particle distribution function. This is of course just the beginning of an infinite hierarchy, since an equation for the two-particle function involves a three-particle function, and so on. The usual procedure is then to truncate this hierarchy in one of a variety of possible ways to obtain a small closed set of reaction–diffusion equations [8]. These equations are necessarily approximate, although they often work quite well.

This seemingly universal limitation to an exact solution of the problem was in fact overcome when attention was shifted from the  $n$ -particle distribution function formulation to a different quantity. In particular, the diffusion-limited coalescence reaction  $A + A \rightarrow A$  was the first of the reactions under discussion here to be solved exactly [3–7]. This became possible because instead of the reactant concentration  $\rho(x, t)$  the problem was formulated in

terms of the *empty interval function*  $E(x, t)$ , defined as the probability that an interval of length  $x$  is empty (contains no particles) at time  $t$ . It is straightforward to deduce that the evolution equation for this function is *exactly* linear,

$$\frac{\partial}{\partial t} E(x, t) = 2D \frac{\partial^2}{\partial x^2} E(x, t), \quad (4)$$

together with the boundary conditions  $E(0, t) = 1$  implied by the coalescence reaction and  $E(\infty, t) = 0$  for any nonvanishing concentration. Here  $D$  is the diffusion coefficient for a reactant particle and the initial condition  $E(x, 0)$  depends on the initial particle distribution. The concentration  $\rho(t)$  and the interparticle distribution function  $P(x, t)$  are immediately obtained from the interval function:

$$\rho(t) = - \left. \frac{\partial E(x, t)}{\partial x} \right|_{x=0}, \quad P(x, t) = \frac{1}{\rho(t)} \frac{\partial^2 E(x, t)}{\partial x^2}. \quad (5)$$

For a random initial distribution of reactants of initial concentration  $\rho(0) = c_0$  the initial interparticle distribution function is of Poisson form,  $P(x, 0) = c_0 \exp(-c_0 x)$  and one readily finds

$$\rho(t) = \rho(0) \exp(2Dc_0^2 t) \operatorname{erfc}[c_0(2Dt)^{1/2}]. \quad (6)$$

Note that this solution is exact for all times in the continuum system, and at long times leads to the anomalous decay  $t^{-1/2}$  also found by a variety of approximate methods [8]. The interparticle distribution function for the random initial distribution of reactants is given by

$$P(x, t) = \frac{c_0}{2} \frac{e^{-c_0 x} \operatorname{erfc}\left[\frac{-x+4c_0 Dt}{(8Dt)^{1/2}}\right] - e^{c_0 x} \operatorname{erfc}\left[\frac{x+4c_0 Dt}{(8Dt)^{1/2}}\right]}{\operatorname{erfc}\left[(2c_0^2 Dt)^{1/2}\right]}. \quad (7)$$

Again, this solution is valid for all times. While it starts out as an exponential, the interparticle distribution function develops a well-known interparticle gap that grows with time and that is responsible for the fact that the reaction slows down relative to the law of mass action. This gap, which reflects the fact that diffusion is a poor mixing mechanism in constrained or low-dimensional geometries, is clear in the analytic scaled asymptotic form obtained from (7) as  $t \rightarrow \infty$  and also found by a variety of approximate methods [8],

$$P(z) = \lim_{t \rightarrow \infty} P(x, t) \frac{dx}{dz} = \frac{\pi}{2} z \exp\left(-\frac{\pi}{4} z^2\right), \quad (8)$$

where  $z = x/(2\pi Dt)^{1/2}$ .

These well known analytic results (which remarkably do not depend on the value of the reaction rate coefficient that would be introduced in the usual reaction–diffusion picture) are a test for our numerical integration scheme in the high  $\gamma$  limit. The integration procedure is described in detail in the appendix. In figure 1 we show the Langevin equation result for the reactant concentration for  $\gamma = 50$  and  $k_B T = 0.2$ . The diffusion coefficient  $D$  in the continuum picture is related to these quantities via the Einstein relation  $D = k_B T/\gamma$  and is thus  $4 \times 10^{-3}$  for the values used in the numerical integration. The figure is on a log–log scale and there are actually four curves in addition to the  $t^{-1/2}$  line, which serves as a guide to the eye. However, only two curves are visible because pairs of curves overlap so precisely that they cannot be distinguished. In particular, the upper curve includes equation (6) (solid) as well as the numerical integration curve (dashed but not visible). The point is that they are *indistinguishable at all times*. Both go to the  $t^{-1/2}$  asymptotic behaviour, but essentially perfect agreement between the reaction–diffusion and Langevin pictures does not require that we go to this limit.

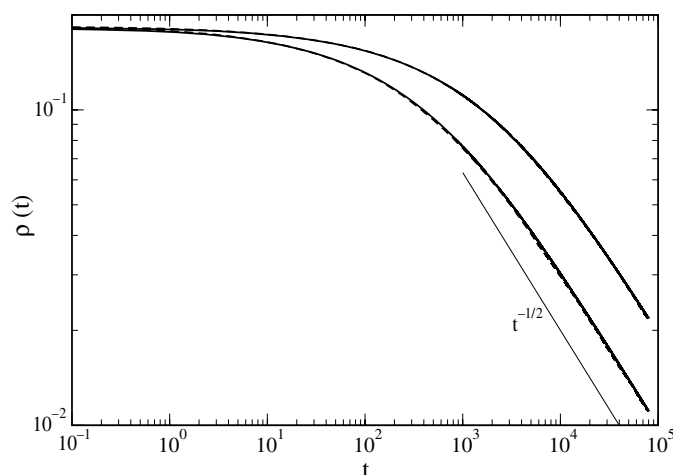


**Figure 1.** Reactant concentration versus time for diffusion-limited reactions. Upper curves:  $A + A \rightarrow A$ ; theory (6) with  $D = 4 \times 10^{-3}$  (solid) and numerical integration (dashed but not visible because of complete overlap). Lower curves:  $A + A \rightarrow \emptyset$ ; theory (11) with  $D = 4 \times 10^{-3}$  (solid) and numerical integration (dashed, again hardly visible). For numerical integration curves:  $\gamma = 50, k_B T = 0.2$ .

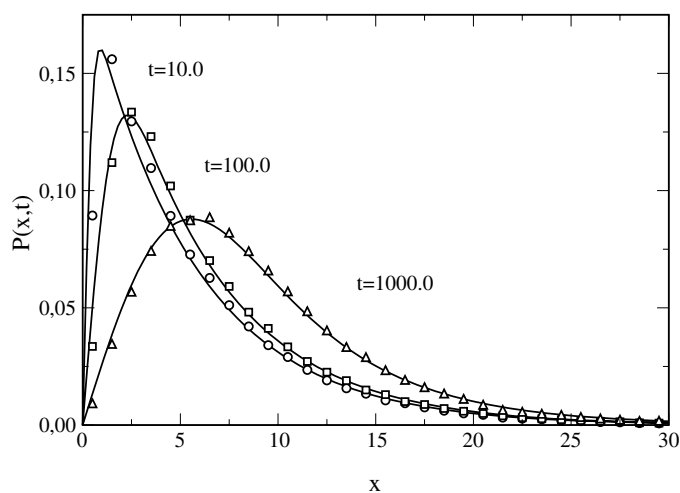


**Figure 2.** Interparticle distribution function for the diffusion-limited coalescence reaction  $A + A \rightarrow A$  at different times. Solid curves: equation (7). Symbols: numerical integration results. Same parameters as in figure 1.

Figure 2 shows the interparticle distribution function  $P(x, t)$  at three different times. The solid curves are obtained from equation (7) and the symbols are the numerical integration results. Again the agreement is excellent. The small differences at the earliest times are due to the finite size of the particles in the numerical integration and the small distortion this causes in the initial distribution, as described in detail in the appendix. The evolution of the interparticle distribution gap that causes the reaction to slow down relative to the mean field behaviour captured by the law of mass action is evident.

The empty interval method cannot be used for the annihilation reaction  $A + A \rightarrow 0$  because the sizes of the empty intervals change discontinuously when there is a reaction. It took a number of years to find another function that could also be calculated exactly and from which physical observables could then be obtained. The problem was finally formulated in terms of the *interval parity function*  $r(x, t)$ , defined as the probability that an interval of length  $x$  contains an even number of particles at time  $t$  [1, 2]. This quantity again evolves *exactly* according to the same linear equation as the empty interval function,

$$\frac{\partial}{\partial t} r(x, t) = 2D \frac{\partial^2}{\partial x^2} r(x, t), \quad (9)$$

but now with boundary conditions  $r(0, t) = 1$  (as for the empty interval) and  $r(\infty, t) = 1/2$ . The concentration is related to the interval parity function precisely as in equation (5),

$$\rho(t) = - \left. \frac{\partial r(x, t)}{\partial x} \right|_{x=0}, \quad (10)$$

but it is not possible to relate the interparticle distribution function to  $r(x, t)$  in any straightforward way so that here the only computable observable is the concentration. For a random initial distribution of reactants one finds

$$\rho(t) = \rho(0) \exp(8Dc_0^2 t) \operatorname{erfc}[2c_0(2Dt)^{1/2}]. \quad (11)$$

The lower curve in figure 1 shows this result as well as the Langevin equation integration outcome. Again, they are perfectly superposed, so only one curve is visible. The asymptotic behaviour is again of the form  $t^{-1/2}$ , the total concentration here being lower because each reaction event eliminates two particles rather than just one. The Langevin equation integration again leads to an interparticle distribution very much like that of figure 2, but we do not show it here because there are no exact analytic results to compare it to.

The exact results obtained for the diffusion-limited  $A + A \rightarrow P$  reaction from the interval approaches are of course well known. That the Langevin approach leads to results that agree with these results provides a test of the suitability of this approach in one parameter regime.

### 3. Ballistic reactions

We now turn to reactants that move ballistically, to compare the predictions made for these cases with the results obtained from the integration of the equations of motion together with the encounter reaction rules when we set the damping equal to zero,  $\gamma = 0$ . Note that there are no exact analytic results for these reactions. In fact, in general the kinetic equations used for their description are themselves approximate, as are the solutions of these equations.

The reaction  $A + A \rightarrow \emptyset$  has been studied in some detail when the initial velocity distribution is dichotomic (and remains dichotomic for all time since annihilation of pairs of particles with opposite velocities does not affect the distribution). The behaviour of the reactant concentration as a function of time in this case has been shown to decay asymptotically as  $\rho(t) \sim t^{-1/2}$ , as in the diffusion-limited case, but for entirely different physical reasons [9, 10, 12, 13]. This result has been obtained by a variety of arguments and has been confirmed via Monte Carlo and molecular dynamics simulations [10, 11, 14–17, 19]. The basic reason for the non-classical behaviour here is reflected in the correlations that develop in the velocities of neighbouring particles, correlations that lead to the inapplicability of the Boltzmann equation in this case. The correlations arise because as time proceeds, nearest neighbouring particles that travel toward one another react, leaving behind particles that travel away from one another or in the same direction (and that eventually react with another partner). The reaction  $A + A \rightarrow \emptyset$  has also been studied for continuous initial velocity distributions. In

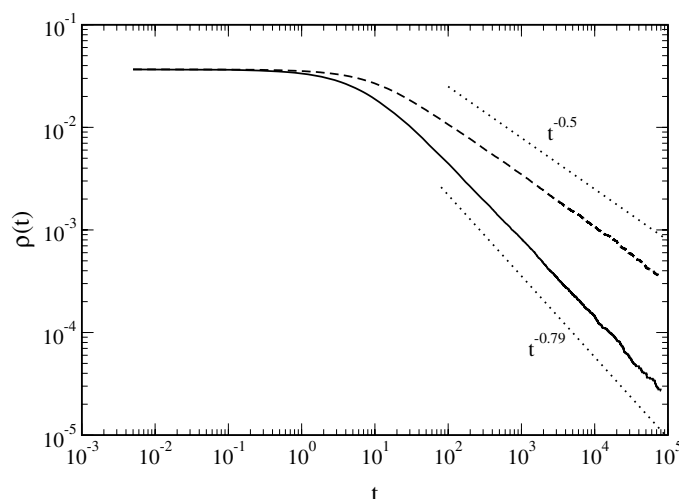


**Figure 3.** Reactant concentration versus time for the ballistic reaction  $A + A \rightarrow \emptyset$  as obtained from the Langevin integration scheme. Dashed curve: dichotomous velocity distribution  $\pm v$  with  $v = 0.2$ . Solid curve: initial Gaussian velocity distribution of width 0.2. The dotted lines are guides for the eye.

this case the Boltzmann equation theories are more successful than in the dichotomous velocity distribution case. The distribution of velocities changes as time proceeds because the fastest reactants have a greater probability of reacting first. The asymptotic decay of the reactant concentration is determined by the slowest particles and hence by the exponent  $\mu$  in the initial velocity distribution near the origin,  $p(v \rightarrow 0) \sim |v|^\mu$  [10, 11, 14–19]. In particular, the Maxwell–Boltzmann distribution in one dimension is a Gaussian, for which  $\mu = 0$ . The theoretical analyses as well as a number of numerical simulations [10, 11, 14, 15, 19] lead to decays  $\rho(t) \sim t^{-\xi}$  with a fair variation in the reported values of  $\xi$ , e.g., 0.666 [10, 11, 14], 0.769 [15], and 0.805 [19]. These values are in any case non-classical, a behaviour that is reflected in the spatial distribution of reactants (see below).

In figure 3 we show  $\rho(t)$  as obtained from our numerical integration for both of these initial velocity distributions. As in the previous section, the initial distribution of positions is random except for the restriction on the overlap of particles described in the appendix, a restriction that might affect some very early time results. The dashed line is the concentration for the dichotomous velocity distribution, and the solid line for the Gaussian distribution. The dotted lines are guides for the eye. The numerical integration scheme leads to the correct asymptotic decay of the concentration in the dichotomous case,  $t^{-1/2}$ . For the Gaussian velocity distribution the decay is certainly within the range of values that have been reported in the literature, close to 0.79. We note that the Langevin scheme is a faster and easier method than are Monte Carlo simulations, and so if sufficiently motivated we could easily push it to obtain a more precise prediction for the value of the decay exponent.

The  $A + A \rightarrow A$  reaction is, as mentioned earlier, a rather artificial one chosen for mathematical convenience rather than physical relevance. Here it requires specification of the velocity of the product. Conservation of momentum would be the most physical criterion. However, in the existing literature [13] a different rule, which conserves momentum *on average*, has also been used, namely, that the product  $A$  has the velocity of one or the other of the reacting pair with probability 1/2. We have adopted this rule in our integration. The asymptotic



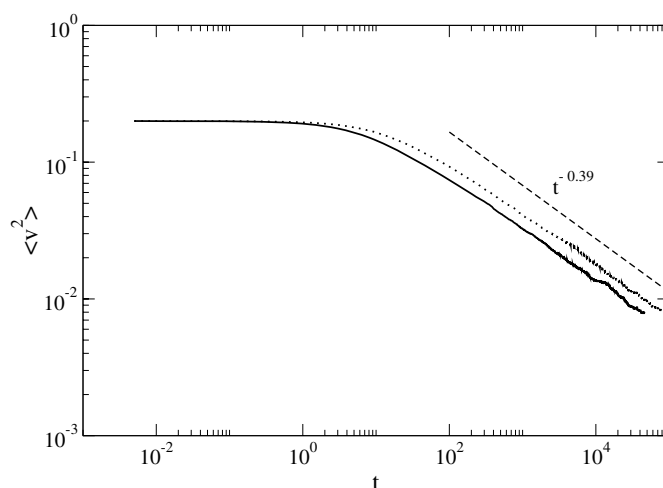


**Figure 4.** Numerical integration results for the root mean square velocity for ballistic reactions with an initial Gaussian distribution. Initial width is 0.2. Solid:  $A + A \rightarrow \emptyset$ . Dotted:  $A + A \rightarrow A$ .

exponents in this case are identical to those in figure 3, but with a concentration that is altogether higher at any given time because each reaction event removes only one reactant particle instead of two.

As the reaction proceeds and the concentration of reactant decays with time, one can also follow the changes in the velocity distribution of the reactants. A dichotomous velocity distribution remains unchanged in time for the  $A + A \rightarrow \emptyset$  reaction. For  $A + A \rightarrow A$  there may be very small unimportant fluctuations created by the survival rule we have implemented, but on average the distribution also remains unchanged. The situation is of course different with a continuous velocity distribution. In the Gaussian case, for both reactions we observe the expected decay of the high velocity wings and the overall narrowing of the distribution, reflecting the faster reaction of faster reactants and the overall consequent cooling of the system. The quantity usually reported as a measure of this progression is the exponent  $\alpha$  in the decay of the root mean square velocity,  $\langle v^2 \rangle^{1/2} \sim t^{-\alpha}$ . There is fairly universal agreement based on theoretical and numerical results that for the annihilation reaction  $A + A \rightarrow \emptyset$  there is a sum rule involving this exponent and that of the concentration decay,  $\alpha + \xi = 1$ . Since one finds a range of values of  $\xi$  in the literature, there is a corresponding range of values of  $\alpha$ . In figure 4 we show our integration results for  $\langle v^2 \rangle$  along with a  $t^{-0.39}$  line (corresponding to  $\alpha = 0.2$ ) to guide the eye. Our results are consistent with the sum rule and, again, we could easily find a more precise value for the decay exponent. Furthermore, the exponents are the same for both reactions, although the mean square value of the velocity is at all times higher for the coalescence reaction. This latter observation is again consistent with the fact that only one reactant is lost per reaction event in this reaction.

Finally, in parallel with the discussion of the diffusion-limited cases of the previous section, we next display the spatial distribution of reactants as the reaction proceeds. We have not found a discussion of these distributions for ballistic reactions, and so there are no predictions with which to compare our results.

The profound differences in the behaviour of the spatial distributions for the different initial velocity distributions are seen in figures 5 and 6. In view of the different asymptotic decay of the concentrations for different velocity distributions exhibited in figure 3, this disparity

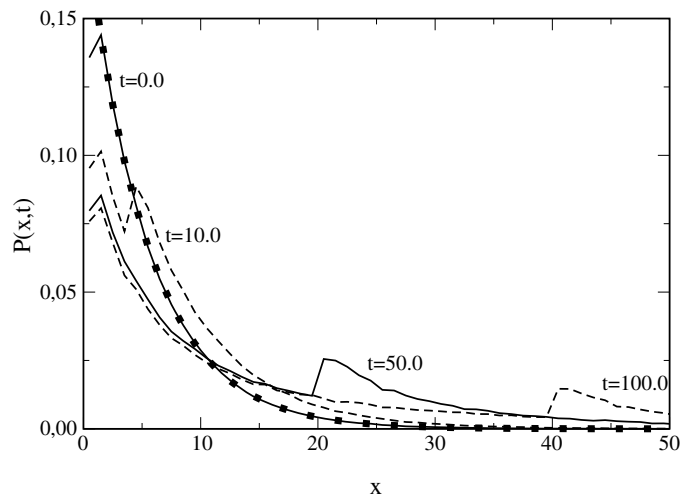


**Figure 5.** Numerical integration results for the interparticle distribution function at different times for the ballistic annihilation reaction  $A + A \rightarrow \emptyset$ . The reactants have a dichotomous velocity distribution,  $\pm v$ , with  $v = 0.2$ .

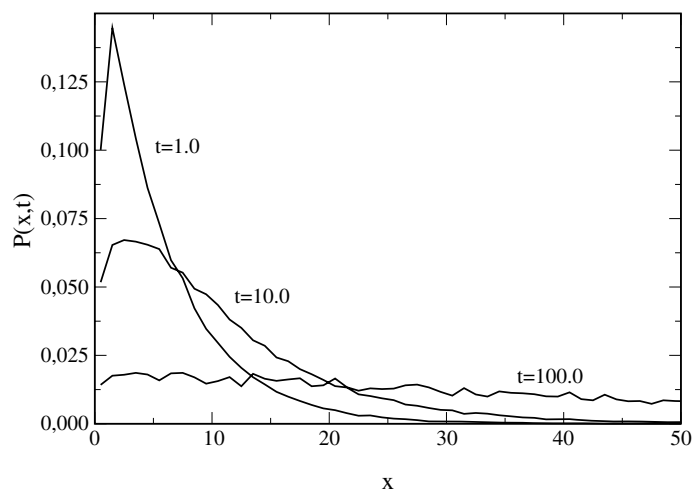


**Figure 6.** Numerical integration results for the interparticle distribution function at different times for the ballistic annihilation reaction  $A + A \rightarrow \emptyset$ . The reactants initially have a Gaussian velocity distribution of width 0.2.

is not surprising. In figure 5 we show the interparticle distribution function for the reaction  $A + A \rightarrow \emptyset$  obtained from the Langevin scheme at zero temperature and zero friction for particles with a dichotomous velocity distribution with velocities  $\pm v$ . The distribution function as a function of interparticle distance is shown for various times for  $v = 0.2$ . Several features are noteworthy, and to understand them we should remember that neighbouring pairs of particles separated by a distance  $\Delta x$  can only be moving relative to one another in one of three ways. They can move toward each other, in which case they will annihilate one another in time  $\Delta t = \Delta x/2v$ . These events lead to a decrease in time of the small  $x$  peak in the figure.

The reactants can simply travel together in the same direction, which does not change their interparticle distance (eventually one or the other will be annihilated in a reaction event with a third particle). Or they can move away from one another, the distance between them increasing as  $2vt$  (again, until a reaction event eliminates one or the other). This third possibility is reflected in the moving peak in the figure, which moves a bit more slowly than  $2vt$  because of the other contributions. Thus, this peak is located near  $x \sim 6$  at  $t = 10$  ( $2vt = 4$ ) and has moved to  $x \sim 22$  at  $t = 50$  ( $2vt = 25$ ), and to  $x \sim 42$  at  $t = 100$  ( $2vt = 50$ ). Thus, an important feature of this interparticle distribution is that there is no interparticle gap at any time, that is, as in a random spatial distribution there is a large probability that the interparticle separation is small (the small ‘gaplet’ at very short distances is again due to the finite size of the particles and the overlap constraint that we place on their initial positioning, as explained in the appendix). One might be tempted to conclude that ballistic motion is an effective mixing mechanism, but mixing is not the source of near particles here. Rather, it reflects the persistence of close neighbours that travel with the same velocity. The concentration decay is anomalous in spite of the ‘Poisson-like’ form of the distribution at short distances because of the velocity correlations described earlier. The other important feature of the interparticle distribution is the moving peak, which is peculiar to a dichotomic (or, in general, a discrete) velocity distribution. Finally we note that the interparticle distribution function for the coalescence reaction  $A + A \rightarrow A$  shows all the same qualitative features as in figure 5.

Figure 6 shows the interparticle distribution function for the reaction  $A + A \rightarrow \emptyset$  obtained from the Langevin scheme at zero temperature and zero friction for particles with an initial Gaussian velocity distribution of width 0.2. This distribution should be compared with figure 2 for a diffusion-limited reaction and figure 5 for the ballistic dichotomous velocity distribution reaction. In the former the interparticle gap discussed earlier implies an almost periodic distribution of reactants. In the latter the distribution retains a Poisson character at all times augmented by the additional peak associated with the velocity correlations. In the continuous velocity distribution case the distribution is different from these two, and evolves toward one that is essentially *homogeneous*, that is, one in which all interparticle distances become equally probable. We are not aware of such a distribution in any other binary reaction problem. The anomalous decay of the concentration reflects this spatial distribution. Again, the interparticle distribution function for the coalescence reaction  $A + A \rightarrow A$  shows all the same qualitative features as in figure 6, with some differences in the detailed timescale to arrive at an essentially uniform distribution.

#### 4. Conclusions

As stated earlier, our overall goal is to establish a general encompassing approach to the binary reaction problem that can subsume known results in appropriate limits, and that can then be used to explore regimes that have not been studied. Our approach is to describe the motion of reactants via an ordinary Langevin equation of motion together with a hard-sphere criterion for the occurrence of reaction events. We proposed that the known diffusion-limited reaction results should be recovered from our formulation in the high friction limit, and that the known ballistic reaction results should correspond to the zero friction limit. We confirmed these propositions for the  $A + A \rightarrow \emptyset$  (annihilation) and  $A + A \rightarrow A$  (coagulation) reactions in one dimension, finding excellent agreement with known results and providing new results even in these limits.

Our next tasks in this programme include an analysis of the  $A + A$  and also the frequently studied  $A + B$  reactions for all ranges of friction and temperature, inclusion of reverse steps and/or additional steps in the reaction mechanism, and extensions to higher dimensions.

Beyond this, we plan to include a possible substrate potential, which is a straightforward addition in a Langevin picture.

### Acknowledgments

This work was supported by the MCyT (Spain) under project FIS2006-11452 (JMS and AML), by CONACYT-Mexico project J-42647-F (AHR), and by the National Science Foundation under grant No. PHY-0354937 (KL).

### Appendix

In this appendix we provide some of the details of our numerical solution of the set of Langevin equations (1), one for each particle, and the implementation of the reaction scheme between particles.

Particles are initially embedded in a system of finite size  $L$  with a given concentration determined by the number of particles placed in the system. In particular, we have taken  $L = 524\,288$  and  $N = 100\,000$ , which corresponds to an initial concentration of  $\rho(0) = c_0 = 0.1907$ . To test for system size effects (and to avoid such effects), in some cases we have increased both  $L$  and  $N$  by the same factor so as to preserve this initial concentration. We implement periodic boundary conditions, so that a particle that leaves the system from one end re-enters it at the other. All the particles have unit mass, and each particle has a radius  $R = 0.1$ . A reaction is defined to occur if the distance between the centres of two particles falls below a particle diameter (since integration updates take place at discrete times, particles may interpenetrate during one integration step). A comment on this particular choice of  $R$  is in order. It must be sufficiently large so that in one integration step of time  $\Delta t$  the Langevin dynamics do not move the particles so far that they are likely to ‘cross’ paths through each other, i.e., we must choose so that  $\langle v^2 \rangle^{1/2} \Delta t \ll 2R$ . Here  $\langle v^2 \rangle^{1/2}$  is the root mean square velocity of the ensemble, used as a measure of the ‘typical’ velocity. On the other hand, for comparison with diffusion and kinetic theories  $R$  must be sufficiently small so that the spatial distribution is minimally distorted by finite particle size effects when compared to continuum particle densities. We have ascertained that the chosen  $R$  meets these requirements, and that changing it within reasonable bounds does not materially affect our results. For the reaction  $A + A \rightarrow \emptyset$  the particles simply disappear upon encounter. For  $A + A \rightarrow A$  the velocity of the surviving particle is randomly chosen to be that of either of the reacting pair with probability  $1/2$  each (additional discussion of this point can be found in section 3).

Initially the particles are deposited randomly in the interval aside from the fact that we do not allow particle overlap. If we did allow overlap, the initially overlapping pairs would react immediately and a considerable number of particles would disappear, thus effectively reducing the initial concentration. Not allowing an overlap causes our distribution to differ from a continuous Poisson form only at very small interparticle distances, which affects the evolution of the distribution only for very short times. We indicate this effect in our simulation results in the main body of the paper as appropriate. The particles have an initial velocity distribution  $P(v, 0)$  of one of two forms, both of which have average velocity  $\langle v \rangle$  equal to zero. One is a binary velocity distribution, where each particle has velocity of magnitude  $v_0$  but with an equal number moving left and right. The other is a Maxwell–Boltzmann distribution whose root mean square,  $\langle v^2 \rangle$ , can be associated with an ‘initial temperature’ of the system.

Once the particles are deposited on the line, we numerically integrate the Langevin equation for each particle using the Heun method, which is an extension of a second order

Runge–Kutta algorithm for stochastic differential equations [22]. The time step is  $\Delta t = 0.005$ , which we ascertain to be sufficiently small for the desired accuracy of our results. After each integration step we check for all pairs of particles that are sufficiently close (overlapping) and allow them to react. To improve the speed of this procedure, we have implemented the ‘method of the neighbouring list’, which assigns particles to pre-defined boxes. Only particles within the same box and in neighbouring boxes are considered when checking for reactive configurations. The neighbouring list is updated every ten iterations.

As the integration and reaction steps proceed, we keep track of all particle positions and velocities and associated histograms, and continue until the number of particles becomes smaller than a predetermined number or until a predetermined maximum time is reached.

## References

- [1] Habib S, Lindenberg K, Lythe G and Molina-París C 2001 *J. Chem. Phys.* **115** 73
- [2] Masser T O and ben-Avraham D 2001 *Phys. Rev. E* **64** 062101
- [3] Doering C R and ben-Avraham D 1988 *Phys. Rev. A* **38** 3035
- [4] Doering C R and ben-Avraham D 1989 *Phys. Rev. Lett.* **62** 2563
- [5] Burschka M A, Doering C R and ben-Avraham D 1989 *Phys. Rev. Lett.* **63** 700
- [6] ben-Avraham D, Burschka M A and Doering C R 1990 *J. Stat. Phys.* **60** 695
- [7] ben-Avraham D 1998 *Phys. Rev. Lett.* **81** 4756
- [8] Lin J-C, Doering C R and ben-Avraham D 1990 *Chem. Phys.* **146** 355
- [9] Elskens Y and Frisch H L 1985 *Phys. Rev. A* **31** 3812
- [10] Ben-Naim E, Krapivsky P, Leyvraz F and Redner S 1994 *J. Phys. Chem.* **98** 7284
- [11] Ben-Naim E and Redner S 1993 *Phys. Rev. Lett.* **70** 1890
- [12] Piasecki J 1995 *Phys. Rev. E* **51** 5535
- [13] Blythe R A, Evans M R and Kafri Y 2000 *Phys. Rev. Lett.* **85** 3750
- [14] Krapivsky P L and Sire C 2001 *Phys. Rev. Lett.* **86** 2494
- [15] Trizac E 2002 *Phys. Rev. Lett.* **88** 160601
- [16] Trizac E 2002 *J. Phys.: Condens. Matter* **14** 2159
- [17] Piasecki J, Trizac E and Droz M 2002 *Phys. Rev. E* **66** 066111
- [18] Coppex F, Droz M and Trizac E 2004 *Phys. Rev. E* **69** 011303
- [19] Lipowski A, Lipowska D and Ferreira A L 2006 *Phys. Rev. E* **73** 032102
- [20] Sancho J M, Romero A H, Lacasta A M and Lindenberg K 2006 in preparation
- [21] Leyvraz F 2003 *Phys. Rep.* **383** 95–212
- [22] Toral R 1995 *Computational Physics (Lecture Notes in Physics vol 448)* ed P Garrido and J Marro (Berlin: Springer)